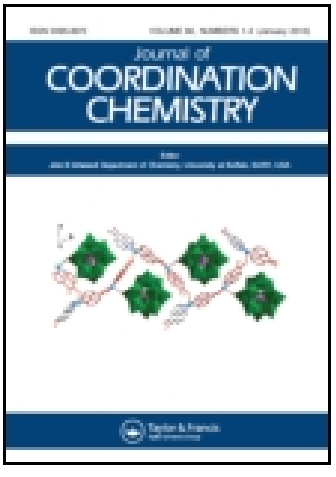

Journal of Coordination Chemistry
Publication details, including instructions for authors and subscription information:
http://www.tandfonline.com/loi/gcoo20

Cadmium(II) complex with 2-methyl-1H-4,5-imidazoledicarboxylic acid ligand: synthesis, characterization, and biological activity

Chi Ma[a], Shi-Kai Liang[a], Fu-Chen Zhao[a], Yang Meng[a], Ying-Ying Li[a], Ming-Chang Zhu[a] & En-Jun Gao[a]

[a] International Key Laboratory of Shenyang Inorganic Molecule-based Chemical, Department of Coordination Chemistry, Shenyang University of Chemical Technology, Shenyang, China

Accepted author version posted online: 29 Sep 2014.Published online: 17 Oct 2014.

To cite this article: Chi Ma, Shi-Kai Liang, Fu-Chen Zhao, Yang Meng, Ying-Ying Li, Ming-Chang Zhu & En-Jun Gao (2014) Cadmium(II) complex with 2-methyl-1H-4,5-imidazoledicarboxylic acid ligand: synthesis, characterization, and biological activity, Journal of Coordination Chemistry, 67:21, 3551-3564, DOI: 10.1080/00958972.2014.970540

To link to this article: http://dx.doi.org/10.1080/00958972.2014.970540

Journal of Coordination Chemistry, 2014
Vol. 67, No. 21, 3551–3564, http://dx.doi.org/10.1080/00958972.2014.970540

Cadmium(II) complex with 2-methyl-1H-4,5-imidazoledicarboxylic acid ligand: synthesis, characterization, and biological activity

CHI MA, SHI-KAI LIANG, FU-CHEN ZHAO, YANG MENG, YING-YING LI, MING-CHANG ZHU and EN-JUN GAO*

International Key Laboratory of Shenyang Inorganic Molecule-based Chemical, Department of Coordination Chemistry, Shenyang University of Chemical Technology, Shenyang, China

(*Received 17 June 2014; accepted 10 September 2014*)

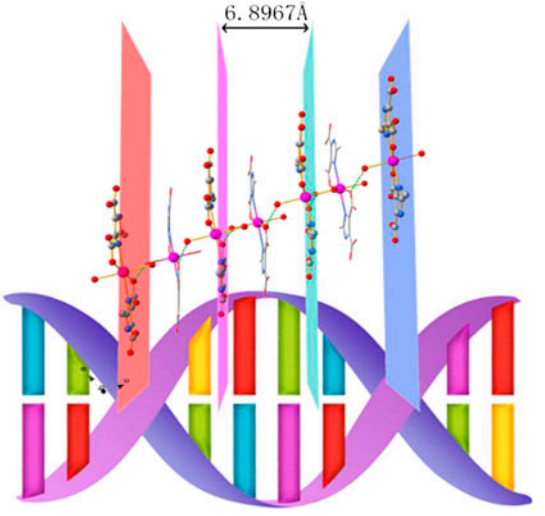

Complex binding to DNA in an intercalative mode

A coordination polymer, $[Cd(L)_2(H_2O)_2]_n$ (HL = 2-methyl-1H-4,5-imidazoledicarboxylic acid), was prepared from reactions of $Cd(NO_3)_2$ with L at room temperature. It was characterized by IR spectra and elemental analysis. The complex was structurally characterized by X-ray single-crystal diffraction revealing that the complex crystallizes in monoclinic with *P2(1)/c* space group, $a = 12.203(10)$ Å, $b = 9.332(8)$ Å, $c = 7.554(7)$ Å, $\beta = 100.894(2)$ Å, $V = 844.7(13)$ Å^3, $Z = 2$. Fluorescence and UV absorption spectroscopy indicated that the complex can bind to fish sperm DNA. Gel electrophoresis assay demonstrated the ability to cleave the HL-60 plasmid DNA. Apoptotic study showed that the complex exhibited significant cancer cell (JEKO and KB) inhibitory rate.

Keywords: Cd(II) complex; DNA binding; Biological activity

*Corresponding author. Email: ejgao@syuct.edu.cn

1. Introduction

Syntheses of coordination polymers have made considerable progress in supramolecular chemistry and crystal engineering [1], for intriguing structural motifs and fascinating topological structures and potential applications in catalysis, molecular adsorption, magnetism, non-linear optics, luminescence, and molecular sensing [2–10]. Recent investigations have addressed the use of the N-heterocyclic dicarboxylate ligands for preparation of coordination polymers due to their versatile coordination and hydrogen-bonding donors and acceptors [11–14]. These studies have demonstrated that 2-methyl-1H-4,5-imidazoledicarboxylic acid (HL) coordinates to metal ions [15–17]. Cd(II) can react with nucleobases, nucleic metallothionein, and plasmid DNA causing extensive damage to these targets [18]. The direct or indirect interaction of Cd(II) complexes with the DNA of cancer cells and their potential anticancer activities were reported as DNA offers some binding sites for cadmium [19–25].

In this article, we report the synthesis and structure characterization of $Cd(L)_2(H_2O)_2$. The interaction with fish sperm DNA (FS-DNA) was examined via fluorescence spectroscopy. Their cleavage behavior toward HL-60 plasmid DNA, cytotoxicity *in vitro,* and apoptosis assays were also investigated.

2. Experimental

2.1. *Materials*

All reagents, solvents and FS-DNA were reagent-grade commercial products and were used without purification. The HL-60 cells, HeLa (human cervix epitheloid carcinoma) cells, KB (human oral epithelial carcinoma) cells, and JEKO-1 (human mantle cell lymphoma) cells were obtained from the Institute of Biochemistry and Cell Biology, SIBS, CAS.

2.2. *Synthesis of the complex*

The compound was prepared from an aqueous solution (20 mL) containing 1.5 mM of HL added dropwise into a water solution (10 mL) of $Cd(NO_3)_2{\cdot}H_2O$ (1.5 mM). KOH (0.2 M L^{-1}) was used to adjust the pH to 6 and then stirred at room temperature. Colorless transparent liquid was obtained from filtration under atmospheric pressure after 12 h. Several weeks later, colorless transparent crystals were obtained and washed with distilled water. Anal. Calcd for $Cd(L)_2(H_2O)_2$ (%): C, 23.65; H, 2.09; N, 11.61; O, 33.15; Cd, 23.29. Found (%): C, 24.07; H, 2.31; N, 11.92; O, 32.62; Cd, 22.08. IR (KBr; v, cm^{-1}): 3240(br), 2620(w), 1720(sh), 1540(m), 1380(m), 1270(sh), 1110(w), 1000(m), 866(m), 773 (m), 675(w) cm^{-1}. CCDC reference number is 1013359.

2.3. *Physical measurements*

Elemental analyses (C, H, and N) were performed with a Finnigan EA 1112 instrument. IR spectra from 400 to 4000 cm^{-1} were recorded on a Nicolet IR 470 spectrophotometer in KBr pellets. UV–visible (UV–vis) spectra were recorded on a Shimadzu UV-240. Fluorescence measurements were performed on a Perkin-Elmer LS55 fluorescence spectrophotometer.

2.4. *X-ray crystallography analysis*

Single-crystal X-ray data of the complex were collected on a Rigaku XtaLAB mini X-ray single crystal diffractometer with MoKα radiation (λ = 0.71073 Å) at 293 K and intensity data were obtained from $3.40° < \theta < 27.53°$ at 273 K by using an ω-scan technique. The structures were solved by direct methods and refined with full-matrix least-squares using SHELXL-97 [26, 27]. Corrections for the least-squares factor and an empirical absorption correction were applied. All non-hydrogen atoms were determined with successive difference Fourier syntheses and refined by full matrix least squares on F^2. Hydrogens were located from difference Fourier maps. Molecular graphics were generated by DIAMOND [28].

2.5. *UV absorption spectroscopy*

UV–visible spectra were recorded on a Shimadzu UV-240. Tris–HCl buffer (pH 7.0) and a buffer (10 mM) solution of complex were titrated with a concentrated FS DNA solution [29].

2.6. *Fluorescence spectroscopic studies*

The buffer used in the binding studies was 50 mM Tris–HCl, pH 7.4, containing 10 mM NaCl. For all fluorescence measurements, the entrance and exit slits were maintained at 10 nm. The sample was excited at 526 nm and the emission range was set between 540 and 750 nm. Under these conditions, the fluorescence intensity of the respective complexes, extracted DNA and ethidium bromide (EtBr) were very small and could be ignored [30].

2.7. *Agarose gel electrophoresis*

For the gel electrophoresis experiments, HL-60 plasmid DNA (0.33 mg mL^{-1}) was treated with the complex in Tris buffer (50.0 mM Tris-acetate, 18.0 mM NaCl buffer, pH 6.8–7.3), and the contents were incubated for 1 h at room temperature. The samples were electrophoresed for 3 h at 90 V on 0.8% agarose gel in Tris-acetate buffer. After electrophoresis, the gel was stained with 1.0 mg mL^{-1} EtBr and photographed under UV light [31].

2.8. *Cell line and culture*

The cell lines used in this experiment were routinely maintained in a RPMI-1640 medium supplemented with 10% (v/v) heat inactivated fetal bovine serum, 2 mM L^{-1} of glutamine, 100 μg mL^{-1} of penicillin, and 100 μg mL^{-1} of streptomycin in a highly humidified atmosphere of 95% air with 5% CO_2 at 37 °C.

2.9. *Cell sensitivity assay*

The growth inhibitory effects of metal complexes on the KB cells and the JEKO-1 cells were measured using the microculture tetrazolium [3-(4,5-dimethylthiazol-2-yl)-2,5-diphenyltetrazolium bromide, MTT] assay. In brief, cells were seeded into a 96-well culture plate at 2×10^5 cells/well in a 100 mL culture medium. After incubation for 24 h, cells were exposed to the tested complexes of serial concentrations. The complexes were dissolved in

DMF and diluted with RPMI 1640 or DMEM to the required concentrations prior to use (0.1% DMF final concentration). The cells were incubated for 24 and 72 h, followed by addition of a 20 μL MTT solution (5 mg mL^{-1}) to each well and further cultivation for 4 h. The media with MTT were removed, and 100 μL of DMSO was added to dissolve the formazan crystals at room temperature for 30 min. The absorbance of each cell at 450 nm was determined by analysis with a microplate spectrophotometer. The IC_{50} values were obtained from the results of quadruplicate determinations of at least three independent experiments.

2.10. *Apoptosis assays by flow cytometry*

The ability of the complex to induce apoptosis is evaluated in JEKO-1 cells and KB cells using Annexin V conjugated with FITC and propidium iodide (PI) counterstaining by flow cytometry. The cells in a usable condition were seeded in a six-well culture plate at 1×10^6 cells per well in a 3 mL culture medium, respectively, in 6 and 12 h later the medium including the Cd(II) complex was given.

After 6 h (or 12 h) incubation, cells were gathered, washed twice with cold phosphate-buffered saline (PBS), and then resuspended in 1× Binging Buffer at a concentration of 1×10^6 cells mL^{-1}. Transferring 100 μL of the solution (1×10^5 cells) to a 5 mL culture tube, 5 μL of FITC Annexin V and 5 μL PI were added. The cells were gently vortex and incubated for 15 min at RT (25 °C) in the dark and then 400 μL of 1× binding buffer was added to each tube before analyzing by flow cytometry (Accuri C6, USA) within 1 h.

2.11. In vitro *apoptosis assay*

Hematoxylin–eosin (H–E) staining was carried out as described previously with some modifications. Briefly, HeLa cells were first grown to 80% confluence on cover slips followed by incubation with 50 μM of the complex for 24 h. Control (untreated), cisplatin, and the complex treated cells were gently washed twice with cold PBS (137 mM NaCl, 2.7 mM KCl, 10 mM Na_2HPO_4, 1.76 mM KH_2PO_4, pH 7.4) and then fixed with 4% paraformaldehyde in PBS for 15 min. Cells were washed three times with PBS, permeabilized with 0.2% Triton X-100 in PBS for 5 min, and washed three times with cold PBS followed by incubation with H–E at 37 °C for 1 h. H–E stained cells were washed three times with cold PBS, mounted on a microscope slide, and visualized under a light microscope fitted with a photometric camera [32].

3. Results and discussion

3.1. *Crystal structures*

The structure of the complex was determined by X-ray crystallography. The crystal data and structure refinement are presented in table 1; selected bond lengths (Å) and angles (°) are listed in table 2.

Single-crystal X-ray analysis revealed that the structure of the complex belongs to the monoclinic system with space group *P2(1)/c*. Cd(II) is six-coordinate (figure 1) by O5 and O5A from water, N1 and N1A and O1 and O1A from two partially deprotonated bidentate HL. The Cd(1)–L (L = O, N of ligand) distances are 2.3122(5)–2.3437(5) Å, while L–Cd–L

Table 1. Crystal data and structure refinement parameters.

Parameter	Value
Formula	$C_{12}H_{10}N_4O_{10}Cd$
Formula weight	482.64
Crystal system, space group	Monoclinic, *P2(1)/c*
a, Å	12.203(10)
b, Å	9.332(8)
c, Å	7.554(7)
β, °	100.984(12)
V, Å^3	844.7(13)
Z	2
ρ_{calcd}, mg cm^3	1.898
Absorption coefficient, mm^{-1}	1.356
Crystal size, mm	0.12 × 0.10 × 0.08
θ Range for data collection, °	3.40–27.53
F (0 0 0)	476
Limiting indices	$-15 \le h \le 15$, $-12 \le k \le 12$, $-9 \le l \le 9$
Reflections collected/unique	8349/1930 [*R*(int) = 0.0435]
Completeness, %	99.5
Data/restraints/parameters	1831/84/132
Goodness-of-fit on F^2	1.089
Final *R* indices [$I > 2\sigma(I)$]	$R_1 = 0.0291$, $wR_2 = 0.0713$
R indices (all data)	$R_1 = 0.0356$, $wR_2 = 0.0745$
Largest diff. peak and hole, e Å^{-3}	0.634 and −0.492

Table 2. Selected bond lengths (Å) and angles (°) for the complex.

Bond	*d*, Å	Bond	*d*, Å
Cd(1)–O(5)	2.271(3)	C(3)–C(4)	1.488(4)
Cd(1)–N(1)	2.312(3)	C(4)–O(4)	1.222(4)
Cd(1)–O(1)	2.343(3)	C(4)–O(3)	1.315(4)
C(1)–O(1)	1.262(3)	C(5)–N(1)	1.332(3)
C(1)–O(2)	1.268(3)	C(5)–N(2)	1.357(4)
C(1)–C(2)	1.488(4)	C(5)–C(6)	1.489(4)
C(2)–C(3)	1.379(4)	O(5)–Cd(1)–N(1)	86.30(10)
C(2)–N(1)	1.381(3)	O(5)–Cd(1)–O(1)	89.34(9)
C(3)–N(2)	1.382(3)	N(1)–Cd(1)–O(1)	72.68(7)

bond angles are 72.684(70) and 107.316(71). The coordination geometry of $[CdN_2O_4]$ is slightly distorted octahedral.

The 1-D chain structure was interconnected by hydrogen-bonding between subunits which include interactions of N(2)···O(4B) and O(4)···N(2B) with bond lengths of 2.8391 Å. As for the 2-D structure (figure 2), the hydrogen bond plays an important role in construction of the 2-D structure [33–35]. The distance between two neighboring Cd ions is 13.0818 Å in the 1-D chain shown by figure 3(b). Figure 3(a) showed that adjacent 2-D structures interacted through hydrogen bonds of the 1-D chain (the distance is 2.8391 Å) to form the 3-D supramolecular architecture. O–H···O and N···O hydrogen bonds were present in the complex as shown in figure 4.

3.2. *UV absorption spectroscopy*

One of the most useful techniques for studying the binding mode of DNA with metal complexes is electronic absorption spectroscopy [36]. Hypochromism and bathochromism occur

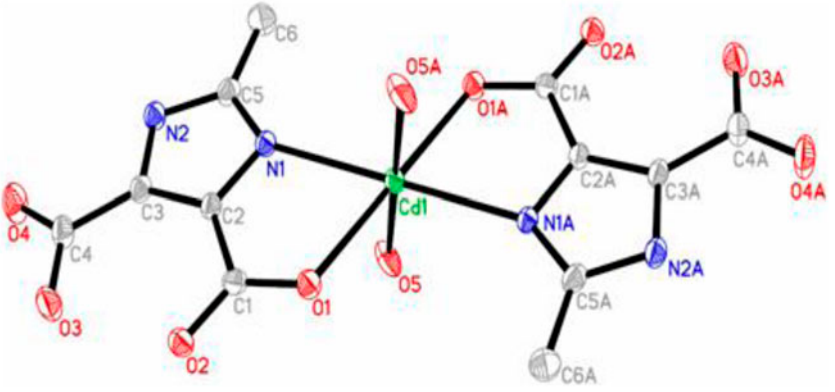

Figure 1. The molecular structure and the local geometry around the metal center and ligand.

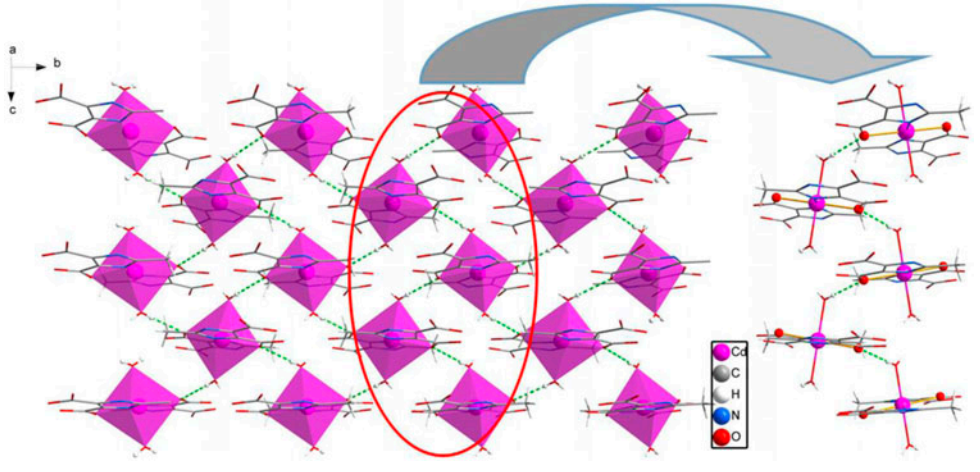

Figure 2. 2-D layer constructed by hydrogen bonds in the compound.

in UV absorption spectroscopy, when a complex binds to DNA through intercalation, due to the coupling π orbital being partially filled by electrons resulting in hypochromism [37]. The π^* orbital of the ligand intercalates with the π orbital of the DNA base pairs resulting in bathochromism. The extent of hypochromism in the UV band is consistent with the strength of intercalative interaction [38–41]. This result suggests that the mode of complex binding to FS-DNA involves a strong stacking interaction between an aromatic group and the base pairs of DNA. The absorption spectra of complex in the absence and presence of FS-DNA are shown in figure 5.

With the presence of increasing FS-DNA to the complex, the slight red shift and hypochromism were observed, which indicates binding of the complex with DNA. The spectral changes have no isosbestic points till the end of the titrations of the complexes with DNA. Thus, there is disequilibrium between DNA bound and free form of the metal complex [42–44].

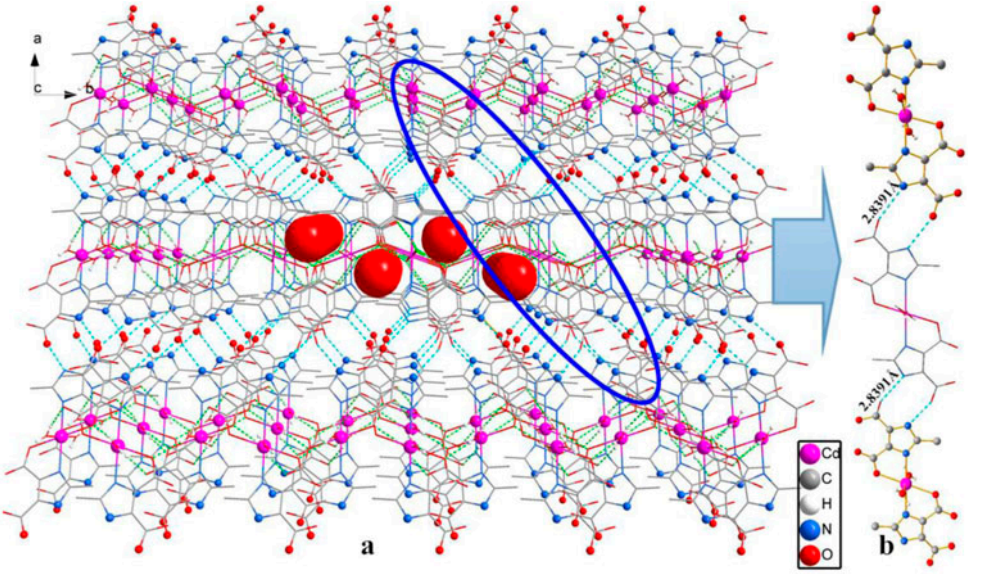

Figure 3. 3-D (a) and 1-D (b) structure of the complex formed by hydrogen-bonding.

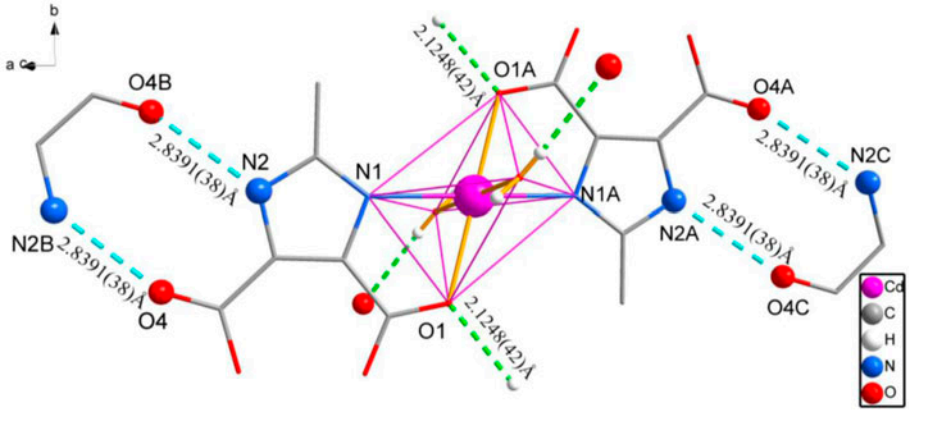

Figure 4. Hydrogen bonds were present in the complex such as O–H···O and N···O.

3.3. *Fluorescence spectroscopic studies*

EtBr is a conjugate planar molecule. Its fluorescence intensity is very weak, but fluorescence emission is greatly increased when in the presence of DNA due to strong intercalation between the contiguous DNA base pairs [43, 45]. The fluorescent light could be quenched by accretion complexes causing decrease in the emission intensity, due to complexes replacing EtBr from DNA [46–49]. Fluorescence quenching measurements can be used to monitor metal binding [50] regardless of their binding modes [51].

The fluorescence emission spectra from addition of the title complex to DNA pretreated with EtBr are depicted in figure 6. Fluorescence intensities at 618 nm (526 nm excitation)

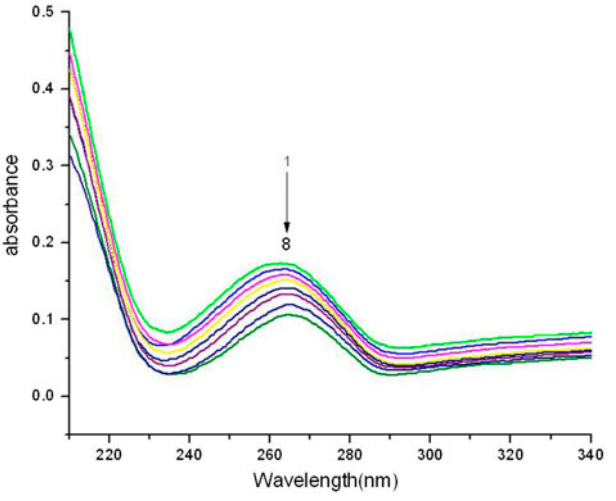

Figure 5. Electronic absorption spectra of the complex in the absence and presence of increasing FS-DNA. Arrow shows the absorbance changes upon increasing DNA.

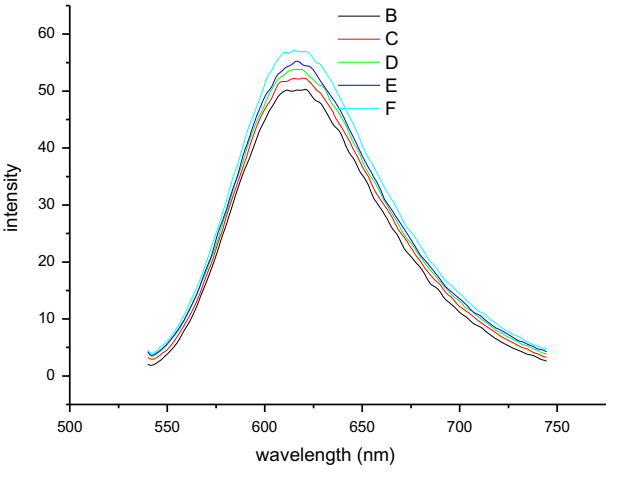

Figure 6. Fluorescence spectra of the binding of EtBr to DNA in the absence (line B) and presence (lines C–F) of increasing amount of the complex.

were measured at different concentrations [52, 53]. Thus, the complex may bind to DNA in an intercalative mode like a regional minor groove binder of DNA (shown in figure 7).

According to the classical Stern–Volmer equation [54]: $I_0/I = 1 + K_{sq}r$, where I_0 and I represent the fluorescence intensities in the absence and presence of the complex, respectively, and r is the concentration ratio of the compound to DNA, K_{sq} is a linear Stern–Volmer quenching constant dependent on the ratio of the bound concentration of EtBr to the concentration of DNA. The K_{sq} value is obtained as the slope of I_0/I *versus* r linear plot. The fluorescence-quenching curve of DNA-bound EtBr by the complex is given in figure 8. The quenching curves illustrate that the complex binds to DNA [55], which indicates that the

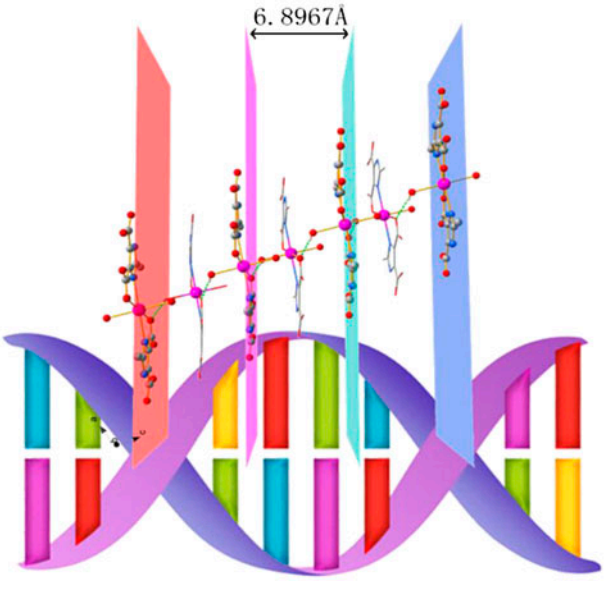

Figure 7. The complex bound to DNA in an intercalative mode.

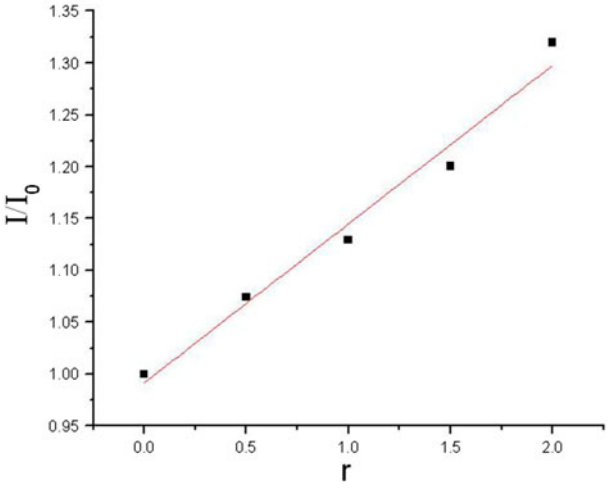

Figure 8. Stern–Volmer quenching plot of the complex.

ability of binding to DNA increases gradually as the concentration ratio of the compound to DNA becomes large.

3.4. *Agarose gel electrophoresis*

The degree to which the complex could function as a DNA cleavage agent was tested using HL-60 plasmid DNA as the target. The efficiency of cleavage of these molecules can be

monitored by agarose gel electrophoresis [56–58]. Intact supercoiled DNA (Form I) under the action of an electric field migrates rapidly, open circular DNA (Form II) migrates slowly [59], and linear DNA migration (Form III) occurs between Forms I and II. The activity of the complex was assessed by the conversion of DNA from Form I to Form II or Form III.

As shown in figure 9, with decreasing concentration of the complex (lanes 2–4), the amount of Form I of HL-60 DNA increased gradually, whereas Form II increased. The greater the concentration, the better cutting results, which is consistent with the tendency in fluorescence properties. So the results indicate that the complex has an effect on DNA cutting [60–63].

3.5. *Cytotoxicity assays*

The *in vitro* growth inhibitory effect of the complex was evaluated in the KB and JEKO-1 cells. The IC_{50} values of the complex are listed in table 3. The complex has higher cytotoxic activity against the JEKO-1 cell line than the KB cell line.

3.6. *Apoptosis assays by flow cytometry*

In 6 and 12 h, respectively, the medium including the Cd(II) complex was given for JEKO-1 cells (figure 10). The experiment is repeated by reproducing the conditions as nearly as possible except that we used KB cells (figure 11). The figure indicates that the number of the dead cancer cells increases gradually with time in early apoptotic (lower right quadrant) or late apoptotic/necrotic (upper right quadrant).

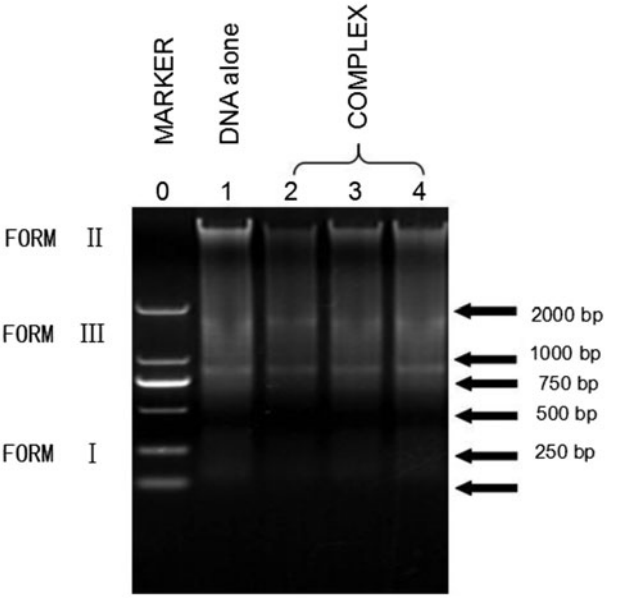

Figure 9. Cleavage of HL-60 DNA (0.5 mg mL^{-1}) in the presence of the complex: Lane 1, DNA alone; Lanes 2–4 at different concentrations of complex: (1) 10 mM; (2) 5 mM; and (3) 2.5 mM.

Table 3. Cytotoxicity of the complex against selected human tumor cells after 24 and 72 h of incubation [data are expressed as mean ± SD (n = 4)].

Time of incubation, h	Tumor cells	*In vitro* activity (IC_{50} (SD, μM)) Complex **1**
24	KB	40 ± 7
	JEKO-1	29 ± 4
72	KB	25 ± 4
	JEKO-1	19 ± 4

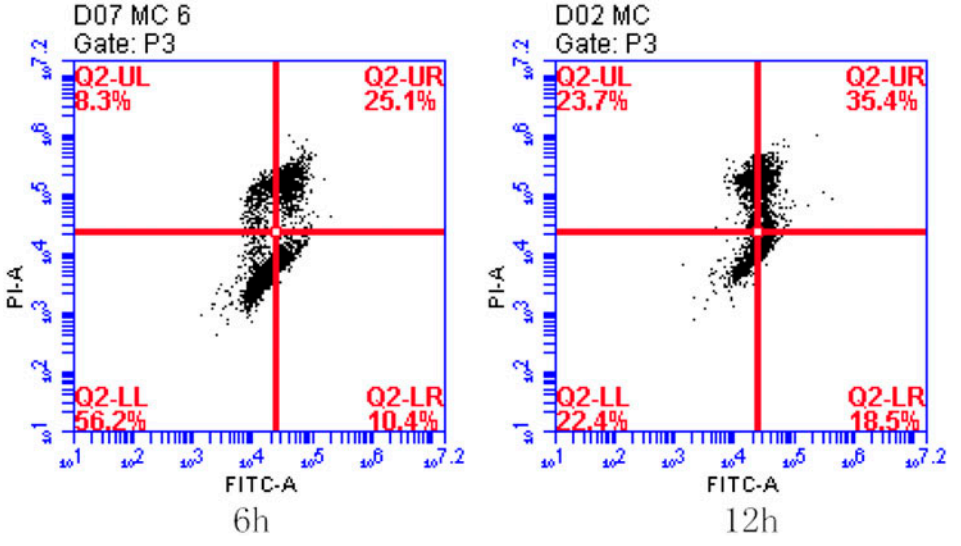

Figure 10. The JEKO-1 cells cultured with 1000 μg mL^{-1} of the complex for 6 and 12 h measured by surface expression of phosphatidyl serine using FITC-conjugated Annexin V antibody. Membrane permeability was assessed by PI exclusion, analyzed by flow cytometry. Dot plots show percentages representing the population of cells that are non-apoptotic (lower left quadrant), early apoptotic (lower right quadrant) or late apoptotic/necrotic (upper right quadrant). Quadrants were established using controls.

3.7. *Apoptotic study*

Apoptosis is the most common occurring gene-controlled process that plays a critical role in tissue homeostasis and elimination of unwanted cells without affecting normal/unaffected cells [64]. To observe in which way the new complexes produced cellular death (necrosis or apoptosis), light microscope studies were performed on KB cells.

The cells stained by H–E were observed and the morphology of the cell nucleus changed obviously in figure 12. In figure 12(a), the normal cells exhibited a dense state and an intercellular tight junction, the single cell has irregular cell morphology and cytoplasm has a clear appearance. Figure 12(b) shows formation of apoptotic bodies in cells treated for 12 h with 50 μM complex where the cell nucleus has become a pyknotic nucleus (shrunken and dark). The nuclear fragmentation indicated that cells are undergoing apoptotic cell death.

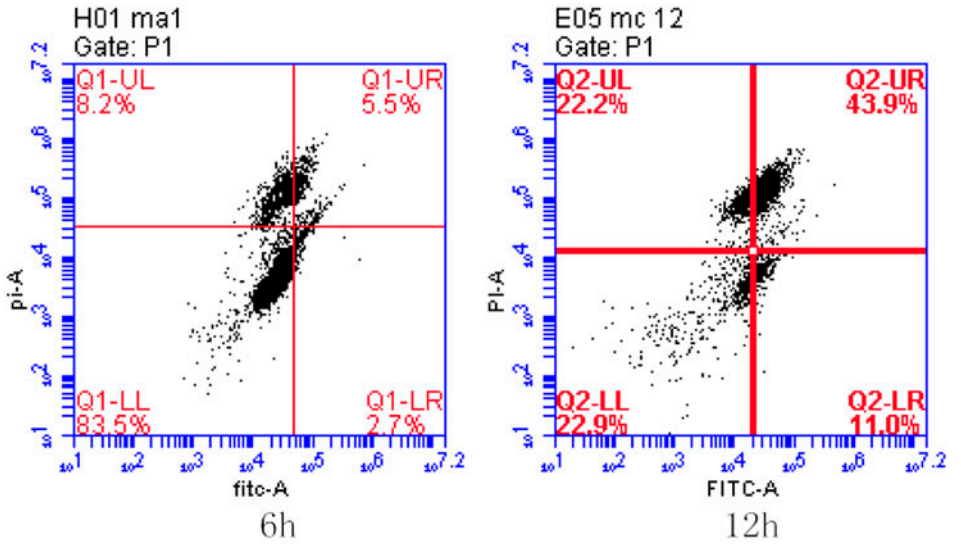

Figure 11. The KB cells cultured with t 1000 μg mL^{-1} of the complex for 6 and 12 h measured by surface expression of phosphatidyl serine using FITC-conjugated Annexin V antibody. Membrane permeability was assessed by PI exclusion, analyzed by flow cytometry. Dot plots show percentages representing the population of cells that are non-apoptotic (lower left quadrant), early apoptotic (lower right quadrant) or late apoptotic/necrotic (upper right quadrant). Quadrants were established using controls.

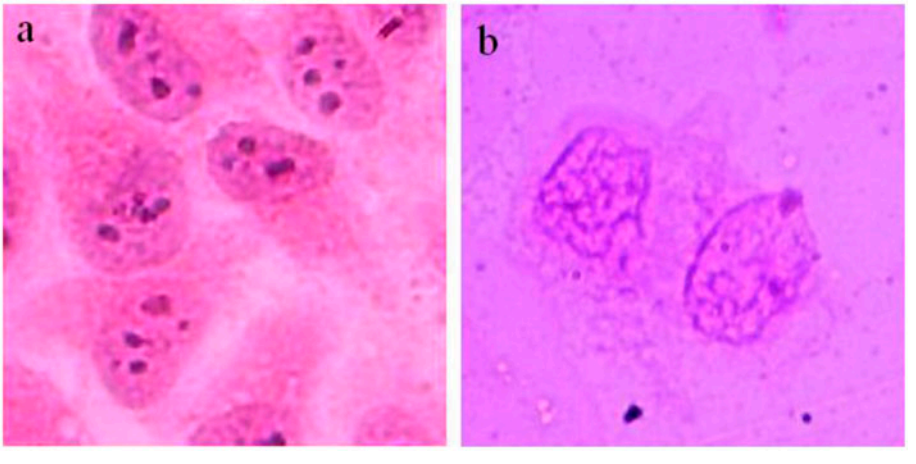

Figure 12. Morphological changes of KB cells. The KB cells were incubated with complex for 12 h, stained with H–E, and visualized under light microscope. (a) Untreated control cells. (b) Cells that were treated with 50 μM of the complex for 12 h.

4. Conclusion

The molecular structure of the complex was determined by single-crystal X-ray diffraction. The DNA binding properties of the complex were examined by fluorescence spectra. The results support the complex binding to DNA through classical intercalation. The capability

of cleavage of extracted HL60-DNA by the complex was investigated using agarose gel electrophoresis and the results also indicated that the complex exhibits DNA-cleavage activity. Cytotoxic and antiproliferative studies show that the complex exhibits cytotoxic activity against KB and the JEKO-1 cells, especially effective against JEKO-1 cell lines. Additionally, apoptotic tests indicated that the complexes had an apoptotic effect on cells tested. Chemical and biological findings indicate that these complexes are promising candidates as live-cell imaging reagents that could contribute to the understanding of cellular uptake of metal complexes.

Acknowledgements

We gratefully acknowledge the Natural Science Foundation of China [grant number 21171118], the Distinguished Professor Project of Liaoning province and the science and technology special fund of Shenyang City (F12-151-9-00).

References

[1] L.A. Borkowski, C.L. Cahill. *Cryst. Growth Des.*, **6**, 2241 (2006).
[2] C.M.G. Dossantos, A.J. Harte, S.J. Quinn, T. Gunnlaugsson. *Coord. Chem. Rev.*, **252**, 2512 (2008).
[3] Y.B. Zhang, W.X. Zhang, F.Y. Feng, J.P. Zhang, X.M. Chen. *Angew. Chem. Int. Ed.*, **48**, 5287 (2009).
[4] B. Moulton, M.J. Zaworotko. *Chem. Rev.*, **101**, 1629 (2001).
[5] S.L. Qiu, G.S. Zhu. *Chem. Rev.*, **253**, 2891 (2009).
[6] M.L. Jain, P.Y. Bruice, I.E. Szabó, T.C. Bruice. *Chem. Rev.*, **112**, 1284 (2012).
[7] A. Garoufis, S.K. Hadjikakou, N. Hadjiliadis. *Coord. Chem. Rev.*, **253**, 1384 (2009).
[8] J. Ruiz, J. Lorenzo, C. Vicente, G. López, J.M. López-de-Luzuriaga, M. Monge, F.X. Avilés, D. Bautista, V. Moreno, A. Laguna. *Inorg. Chem.*, **47**, 6990 (2008).
[9] E.J. Gao, L. Lin, L. Liu, M.C. Zhu, B. Wang, X.N. Gao. *Dalton Trans.*, **41**, 11187 (2012).
[10] E.J. Gao, C. Liu, M.C. Zhu, H.K. Lin, Q. Wu, L. Liu. *Anti-Cancer Agents Med. Chem.*, **9**, 356 (2009).
[11] Z.G. Gu, Y.T. Liu, X.J. Hong, Q.G. Zhan, Z.P. Zheng, S.R. Zheng, W.S. Li, S.J. Hu, Y.P. Cai. *Cryst. Growth Des.*, **12**, 2178 (2012).
[12] Y.L. Wang, D.Q. Yuan, W.H. Bi, X. Li, X.J. Li, F. Li, R. Cao. *Cryst. Growth Des.*, **5**, 1849 (2005).
[13] W.G. Lu, C.Y. Su, T.B. Lu, L. Jiang, J.M. Chen. *J. Am. Chem. Soc.*, **128**, 34 (2006).
[14] X.F. Wang, X.Y. Yu, J.K. Hu, H. Zhang. *J. Coord. Chem.*, **66**, 2118 (2013).
[15] G.M. Sheldrick, *SHELXL 97: Program for the Refinement of Crystal Structures*, University of Gottingen, Germany (1997).
[16] G.M. Sheldrick. *Acta Cryst. A*, **64**, 112 (2008).
[17] T. Li, Y. Xiu, X. Su, X.R. Meng. *J. Coord. Chem.*, **65**, 3111 (2012).
[18] N.A. Illán-Cabeza, R.A. Vilaplana, Y. Alvarez, K. Akdi, S. Kamah, F. Hueso-Ureña, M. Quirós, F. González-Vílchez, M.N. Moreno-Carretero. *J. Biol. Inorg. Chem.*, **10**, 924 (2005).
[19] R. Manikandan, N. Chitrapriya, Y.J. Jang, P. Viswanathamurthi. *RSC Adv.*, **3**, 11647 (2013).
[20] Z. Hossain, F. Huq. *J. Inorg. Biochem.*, **90**, 97 (2002).
[21] Z. Hossain, F. Huq. *J. Inorg. Biochem.*, **90**, 85 (2002).
[22] P.A. Ochoa, M.I. Rodríguez-Tapiador, S.S. Alexandre, C. Pastor, F. Zamora. *J. Inorg. Biochem.*, **99**, 1540 (2005).
[23] X.F. Li, L.R. Rong, H.L. Yi. *Nat. Sci. Ed.*, **27**, 292 (2004).
[24] F.J. Yin, H. Zhao, X.Y. Xu, M.W. Guo. *J. Coord. Chem.*, **66**, 3199 (2013).
[25] D.L. Hamilton, L.S. Valberg. *Am. J. Physiol.*, **227**, 1033 (1974).
[26] G.M. Sheldrick, *SHELXS 97: Program for the Solution of Crystal Structures*, University of Gottingen, Germany (1997).
[27] G.M. Sheldrick. *Acta Cryst. A*, **64**, 112 (2008).
[28] K. Brandenburg, H. Putz. *DIAMOND*, Crystal Impact GbR, Bonn, Germany (2006).
[29] B.S. Yang, J.Y. Feng, Y.Q. Li, F. Gao, Y.Q. Zhao, J.L. Wang. *J. Inorg. Biochem.*, **96**, 416 (2003).
[30] E.J. Gao, K.H. Wang, X.F. Gu, Y. Yu, Y.G. Sun, W.Z. Zhang. *J. Inorg. Biochem.*, **101**, 1404 (2007).
[31] S.S. Hindo, M. Frezza, D. Tomco, M.J. Heeg. *Eur. J. Med. Chem.*, **44**, 4353 (2009).
[32] R. Shakya, F.Y. Peng, J.G. Liu, M.J. Heeg, C.N. Verani. *Inorg. Chem.*, **45**, 6263 (2006).
[33] S.J. Coles, S.E. Durran, M.B. Hursthouse. *New J. Chem.*, **25**, 416 (2001).

[34] D. Kovala-Demertzi, J.R. Miller, N. Kourkoumelis. *Polyhedron*, **18**, 1005 (1999).
[35] P. Li, Y.C. Qiu. *Inorg. Chem. Commun.*, **10**, 705 (2007).
[36] Q.L. Zhang, J.H. Liu, P.X. Zhang, X.Z. Ren, C.H. Li, W.L. Hong, J.Z. Liu, L.N. Ji. *Chin. J. Inorg. Chem.*, **21**, 344 (2005).
[37] J.G. Liu, Q.L. Zhang, X.F. Shi, L.N. Ji. *Inorg. Chem.*, **40**, 5045 (2001).
[38] L.-M. Chen, J. Liu, J.-C. Chen, C.-P. Tan, S. Shi, K.-C. Zheng, L.-N. Ji. *J. Inorg. Biochem.*, **102**, 330 (2008).
[39] J.-G. Liu, Q.-L. Zhang, X.-F. Shi, L.-N. Ji. *Inorg. Chem.*, **40**, 5045 (2001).
[40] A.M. Pyle, J.P. Rehmann, R. Meshoyrer, C.V. Kumar, N.J. Turro, J.K. Barton. *J. Am. Chem. Soc.*, **111**, 3051 (1989).
[41] X.W. Liu, J. Li, H. Deng, K.C. Zheng, Z.W. Mao, L.N. Ji. *Inorg. Chim. Acta*, **358**, 3311 (2005).
[42] H.M. Torshizi, T.S. Srivastava, S.J. Chavan, M.P. Chitnis. *J. Inorg. Biochem.*, **48**, 1163 (1992).
[43] A. Blake, A.R. Peacocke. *Biopolymers*, **5**, 871 (1967).
[44] A.K. Paul, T.S. Srivastava, S.J. Chavan, M.P. Chitnis, S. Desai, K. Rao. *J. Inorg. Biochem.*, **61**, 179 (1996).
[45] C.-Y. Zhou, J. Zhao, Y.-B. Wu, C.-X. Yin, Yang Pin. *J. Inorg. Biochem.*, **101**, 10 (2007).
[46] B.C. Baguley, M. Le Bret. *Biochemistry*, **23**, 937 (1984).
[47] G.Y. Bai, K.Z. Wang, Z.M. Duan, L.H. Gao. *J. Inorg. Biochem.*, **98**, 1017 (2004).
[48] S.A. Tysoe, R. Kopelman, D. Schelzig. *Inorg. Chem.*, **38**, 5196 (1999).
[49] G.Y. Han, P. Yang. *J. Inorg. Biochem.*, **91**, 230 (2002).
[50] B.S. Yang, J.Y. Feng, Y.Q. Li, F. Gao, Y.Q. Zhao, J.L. Wang. *J. Inorg. Biochem.*, **96**, 416 (2003).
[51] W.-J. Mei, J. Liu, H. Chao, L.-N. Ji, A.-X. Li, J.-Z. Liu. *Transition Met. Chem.*, **28**, 852 (2003).
[52] H. Mansuri-Torshizi, R. Mital, T.S. Srivastava, H. Parekh, M.P. Chitnis. *J. Inorg. Biochem.*, **44**, 239 (1991).
[53] E.J. Gao, X.M. Zhao, Q.T. Liu, R. Xiu. *Acta Chim. Sinica*, **62**, 593 (2004).
[54] J.R. Lakowicz, G. Weber. *Biochemistry*, **12**, 4161 (1973).
[55] H. Arakawa, R. Ahmad, M. Naoui, H.A. Tajmir-Riahi. *J. Biol. Chem.*, **275**, 10150 (2000).
[56] C.Y. Shi, E.J. Gao, S. Ma, M.L. Wang, Q.T. Liu. *Bioorg. Med. Chem. Lett.*, **20**, 7250 (2010).
[57] E.J. Gao, M.C. Zhu, H.X. Yin, L. Liu, Q. Wu, Y.Y. Sun. *J. Inorg. Biochem.*, **102**, 1958 (2008).
[58] T. Ohse, S. Nagaoka, Y. Arakawa, H. Kawakami, K. Nakamura. *J. Inorg. Biochem.*, **85**, 201 (2001).
[59] V. Rajendiran, R. Karthik, M. Palaniandavar, H. Stoeckli-Evans, V.S. Periasamy, M.A. Akbarsha, B.S. Srinag, H. Krishnamurthy. *Inorg. Chem.*, **46**, 8208 (2007).
[60] E.J. Gao, K.H. Wang, X.F. Gu, Y. Yu, Y.G. Sun, W.Z. Zhang, H.X. Yin, Q. Wu, M.C. Zhu, X.M. Yan. *J. Inorg. Biochem.*, **101**, 1404 (2007).
[61] Q.L. Zhang, J.G. Liu, J.Z. Liu, H. Li, Y. Yang, H. Xu, H. Chao, L.N. Ji. *Inorg. Chim. Acta*, **339**, 34 (2002).
[62] X.L. Wang, H. Chao, H. Li, X.L. Hong, Y.J. Liu, L.F. Tan, L.N. Ji. *J. Inorg. Biochem.*, **98**, 1143 (2004).
[63] J. Qian, W. Gu, H. Liu, F.X. Gao, L. Feng, S.P. Yan, D.Z. Liao, P. Cheng. *Dalton Trans.*, **10**, 1060 (2007).
[64] M.C. Alley, D.A. Scudiero, A. Monks, M.L. Hursey, M.J. Czerwinski, D.L. Fine, B.J. Abbott, J.G. Mayo, R.H. Shoemaker, M.R. Boyd. *Cancer Res.*, **48**, 589 (1988).